CORROSION 2014
Collaborate. Educate. Innovate. Mitigate.
March 9-13, 2014 • Henry B. Gonzalez Convention Center • San Antonio, Texas, U.S.A.

Chloride Corrosion Threshold Dependence on Steel Potential in Reinforced Concrete

Andrea N. Sánchez and Alberto A. Sagüés
University of South Florida
Department of Civil and Environmental Engineering
4202 East Fowler Ave.
Tampa, FL 33620 U.S.A.

ABSTRACT

In reinforced concrete structures exposed to marine environments, corrosion initiates when the chloride ion concentration at the surface of the embedded steel bar exceeds a chloride corrosion threshold (C_T) value. C_T is generally assumed to have a conservatively fixed value between 0.2-0.4% by weight of cement. However, over the last 40 years there have been extensive experimental investigations on chloride corrosion threshold confirming that C_T is not a fixed value and depends on many variables, one of which is the potential of the steel while it is in its passive state. Marked increases in C_T are associated with more negative pre-activation potentials. Experimental measurements of the effect can be found in the literature but for a limited set of conditions. Experiments were designed and conducted here for more detailed assessment. The results were analyzed along with previous data to identify trends and corresponding descriptive parameters. A formulation with $C_T = C_{T0} \, 10^{\wedge}(E-E_0)/\beta_{CT}$ was used and values generally consistent with previous tentative trends were obtained.

Key words: chloride corrosion threshold, steel, electric potential, corrosion, concrete, cathodic polarization, cathodic prevention

INTRODUCTION

There is wide scatter of data in the literature on reported values of chloride corrosion threshold, C_T. In some cases that variation is by more than two orders of magnitude. Part of that scatter reflects methodological differences. Nevertheless, conservative values of C_T tend to be adopted for design purposes. Those values typically range between 0.2% and 0.4% by weight of cement for plain carbon steel bars.

Despite the scatter in C_T values and the experimental inconsistency, previous investigations have identified some parameters that more or less consistently affect that the value of C_T.[1-3] Among those are: condition of the steel surface, exposed area of the steel, concrete properties, oxygen availability at the steel surface, temperature, pore solution composition, w/c ratio, type of chloride salt and chloride source, as well as the potential of the steel while in the passive state.[1] This last factor in particular, whereby C_T increases when passive steel is cathodically polarized, has been considerably neglected

and is examined in detail here.[2] The limited information available to date indicates that the C_T dependence on the increase in cathodic polarization may be described in general terms by Equation 1.

$$log_{10}\left(\frac{C_T}{C_{To}}\right) \sim \frac{E_{To}-E}{\beta_{C_T}} \qquad \text{Eq. (1)}^{[4]}$$

where E is the potential of the passive steel bar, β_{CT} is the characteristic inverse slope of the increase of C_T in a E-logC_T representation, and E_{T0} and C_{T0} are constant values.

Chloride ions ingress through the concrete pore network and accumulate on the embedded steel surface. When C_T is exceeded, corrosion initiates shifting the steel potential to more negative values. In the passive regions adjacent to the activation zone, the steel potential drops negatively as well, due to macrocell coupling. Consequently, that negative potential increases the C_T value of the nearby still passive regions and corrosion initiation there tends to take longer to occur. Preliminary corrosion-related damage modeling shows that neglecting that phenomenon can lead to erroneously high damage projections.[5-8] Thus, introduction of the chloride corrosion threshold dependence on potential is a desirable component for accurate forecasting but more information is needed to compensate for the uncertainty, scarcity and scatter of the relevant C_T data.

An experimental assessment made by Alonso et al. was one of the first investigations that focused on the chloride corrosion threshold dependence on potential, finding behavior that agreed with that expected from Equation 1.[2] That work was conducted however with small mortar specimens and fast chloride ingress. It is desirable to establish whether the resulting C_T-E pattern would be similar in more realistic conditions, when chloride buildup takes place by transport through a thicker cementitious material layer including coarse aggregate, and when using a greater rebar exposure area.

Sánchez and Sagüés validated the work by Alonso et al. and supplemented the limited set of available data in the literature through preliminary experimental assessment.[9] Cylindrical mortar specimens with an embedded carbon steel bar were permanently submerged in a saturated NaCl solution and polarized at various conditions. The assessed specimens were greater in size than those tested by Alonso et al, but still relatively small to represent field conditions. Results confirmed that cathodically polarizing passive steel results in an increased chloride threshold, generally following Equation 1.

An investigation by Li et al. found that the surface area of the steel is an influential parameter on the chloride corrosion threshold, the greater the surface area, the smaller the value of C_T.[10] They strongly suggested to test large-sized reinforced concrete specimens rather than assessing typical small scale laboratory experiments. Furthermore, tests with very small scale specimens tend to be conducted with a small concrete cover that leads to a chloride ion penetration governed mainly by permeation rather than diffusion, which is the prevalent mode of ingress of chloride ions in the systems of interest.[11]

Per the previous discussion, more systematic and sophisticated experimental assessments are desirable to address the noted uncertainties, so as to improve the quantification of the chloride corrosion threshold dependence on steel potential. An evaluation of the critical chloride threshold dependence on steel potential is presented here, that includes a large area of steel embedded in concrete, a moderately thick concrete cover, and exposure in wet and dry cycles, which are more representative of actual field conditions.

EXPERIMENTAL PROCEDURE

Materials and experimental setup

A modified version of the ASTM G109 "Standard Test Method for Determining Effects of Chemical Admixtures on Corrosion of Embedded Steel Reinforcement in Concrete Exposed to Chloride Environments" was used as a basis to prepare a set of twelve reinforced concrete slabs 26 in (66 cm) long, 4 in (10.16 cm) wide and 2.5 in (6.35 cm) high, exposed to a ponding regime while under potentiostatic control as shown in Figure 1.[12]
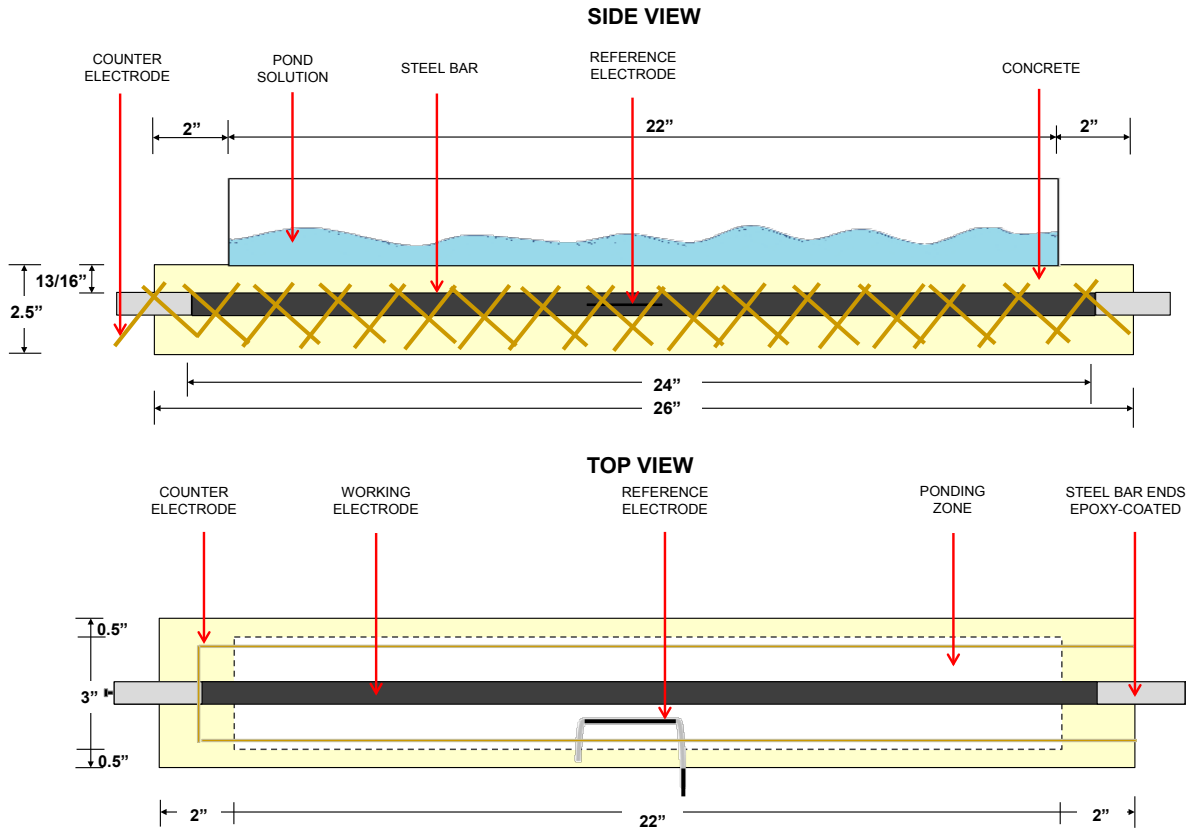
SIDE VIEW

TOP VIEW

Figure 1: Side and top view of the reinforced concrete specimens

The concrete cover thickness X_C of the embedded steel rebar was 0.375 in (2 cm). Only one rebar was used, size #5 plain steel ASTM[(1)] A-615-09B Grade 60 with an undisturbed gray mill scale, with an area of exposure of ~46.5 sq. in. (~300 cm^2), approximately an order of magnitude greater than in previous work.[9] Ordinary Portland Cement Type I/II was used with a water-to-cement ratio (w/c) of 0.6 and a cement-to-sand ratio (c/s) of 2.2. The coarse aggregate used was #89 limestone. The cement factor (CF) was 455 kg/m^3. A set of triplicate specimens were tested at the open circuit potential (OCP) and three additional triplicate sets were cathodically polarized at -0.200, -0.400 and -0.600 V (SCE), respectively.

The reinforced concrete specimens were cured for 32 days at high humidity. After curing, a pond was placed on top of each slab (similarly as in Ref.12) to create wet and dry regimes. Fresh water was ponded continuously during the first 17 days for leak proofing and stabilization. Afterwards, regular wet-dry ponding took place; during the wet cycle (3.5 day period) a solution of 4M NaCl was placed in the pond. The solution was removed for the dry cycle (3.5 days too).

[(1)] American Society for Testing and Materials, ASTM, 100 Barr Harbor Dr, West Conshohocken, PA 19428

The evolution of the steel potential was measured periodically for all the specimens and Electrochemical Impedance Spectroscopy (EIS) tests were performed periodically as well, for the OCP specimens only. A frequency range of 1 mHz to 1 MHz with an amplitude of 0.010 V rms was used. The Echem Analyst[†] software by Gamry[†] Instruments was used to model and estimate the Polarization Resistance (Rp) value of the embedded steel bar. The Rp value was calculated assuming a circuit that has a solution resistance, and a non-ideal interfacial capacitance and polarization resistance parallel combination.

Unlike the specimen configuration in ASTM G-109, the steel bar embedded in each specimen was intended to be cathodically polarized (except those at the OCP condition) with a potentiostat as mentioned above. For that reason, a 2 in (5 cm) embedded activated titanium reference electrode (RE), frequently calibrated with respect to an external SCE, was placed parallel to the steel bar. The counter electrode (CE), a mixed metal oxide (MMO) deposited in a titanium mesh, was placed on either side parallel to the length of the steel bar. The CE was held to plexiglass rods to prevent any contact with the working electrode.

A 2D model using Comsol Multiphysics[†] was developed to find optimal position for the CE placement by minimizing the variability of the potential at the steel surface between the upper and lower arrowed points as illustrated in Figure 2. The modeling results showed that the configuration on the left hand side of the picture, CE placed under the steel bar, resulted in a larger electric potential (red font numbers) difference between the arrowed points compared to the CE configuration on the right hand side. In the latter, the CE placed in a position parallel to the embedded steel bar yielded an electric potential difference as little as ~0.003V, indicating a uniform current flow along the steel bar. Hence, the right side configuration was used to make the specimens as shown earlier.
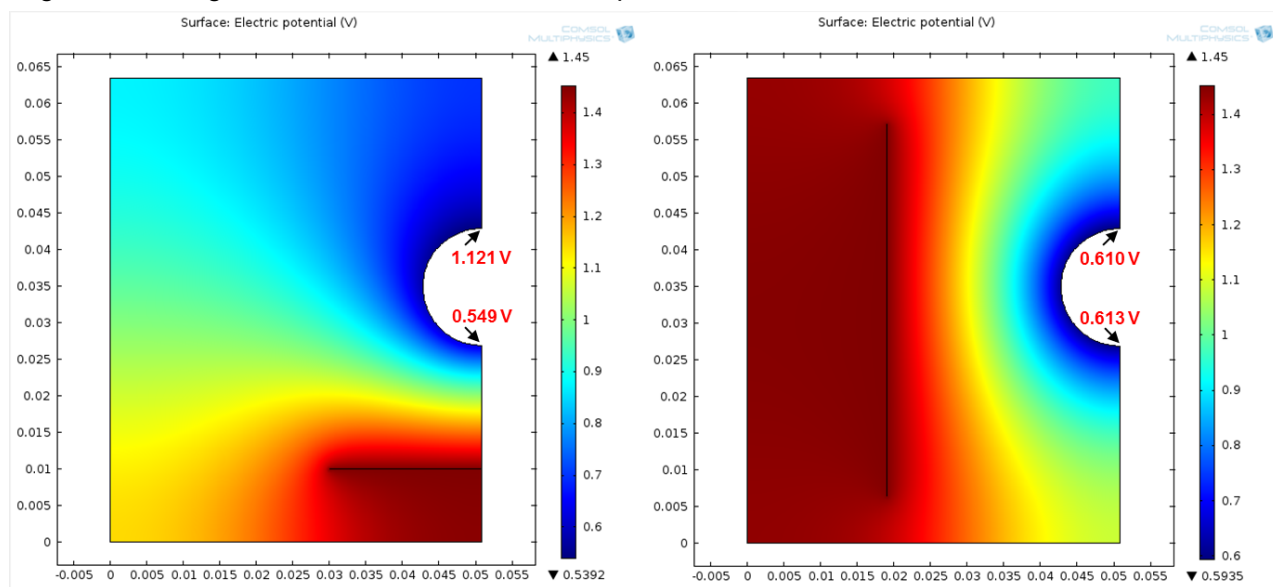

Figure 2: Modeling results to find optimal position for counter electrode placement

RESULTS AND DISCUSSION

Open Circuit Specimens

When the salt water ponding regime exposure was initiated (day zero) the steel potential readings were around -0.080 V vs SCE and remained so for about 150 days as it is shown in Figure 3. The moment of corrosion initiation (or activation) was declared when the steel potential of -0.200 V vs SCE or less was reached. As a secondary confirmation of steel activation, the value of Rp was observed to have exhibited about one order of magnitude decrease compared to the value when the embedded steel was in the passive condition.
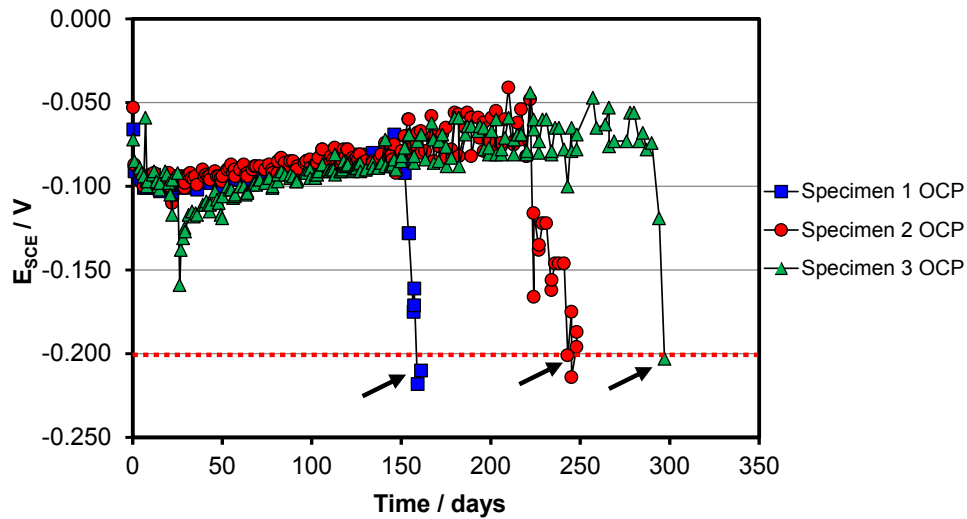

[†] Trade name.

Figure 3: Evolution of the steel potential for the OCP specimens. Arrows indicate activation event declaration.

The activation events for the OCP specimens are indicated by the arrows in Figure 3. The average activation time for the triplicate set was 235 days. The specimens were retained sometime after the activation events occurred to validate corrosion initiation through EIS tests. An example of Nyquist plot results is shown for specimen 1 in Figure 4. During the first 150 days the embedded steel bar maintained an Rp value of ~20,000 ohms. Twenty days later, a potential drop to -0.170 V vs SCE was measured and a pronounced reduction of the semi-circle diameter on the Nyquist plot was observed with an Rp value of ~4000 ohms. The activation time was declared on day 161, when the steel potential passed the -0.200 V mark with a reading of -0.220 V (SCE). EIS test resulted in an Rp of ~2,000 ohms, validating the time of activation estimated from OCP measurements.
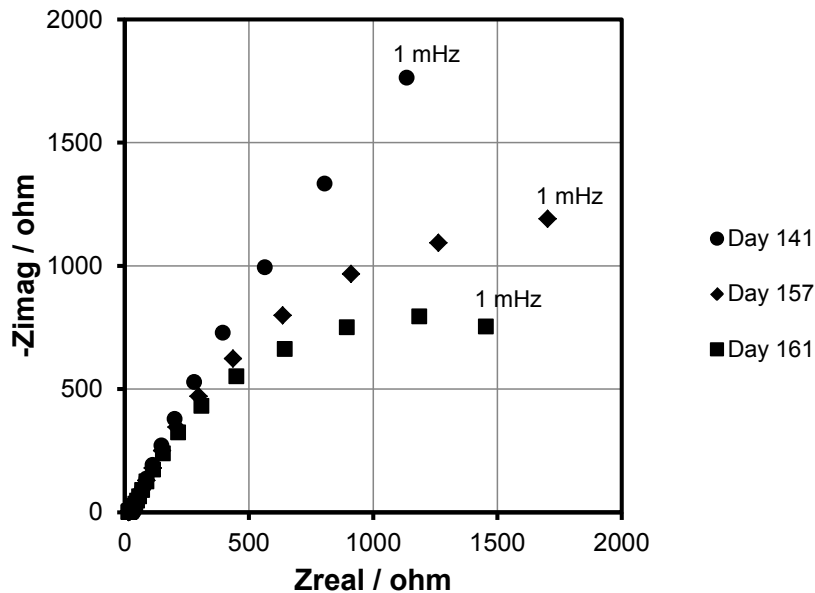

Figure 4: Time progression of EIS for specimen 1 at OCP condition, indicating marked reduction in R_P on activation at day 161. Nyquist representation; 5 data points per frequency decade.

Cathodically Polarized Specimens

The current demanded by the polarized specimens was initially negative (cathodic) when the embedded steel bar potential was set towards negative values (-0.200, -.0.400 and -0.600 V vs SCE). Following the methodology of previous work[9], the moment of activation was declared when the demanding current density reached a value greater than +0.2 µA/cm^2. An example of this procedure for specimen 6, polarized at -0.200 V (SCE) is shown in Figure 5. The red dashed line and the black arrow corresponds to the activation criterion and event, respectively. Fluctuations were observed during the cathodic-anodic current transition as shown in Figure 5, thus specimens were kept polarized for a period afterwards to confirm activation.
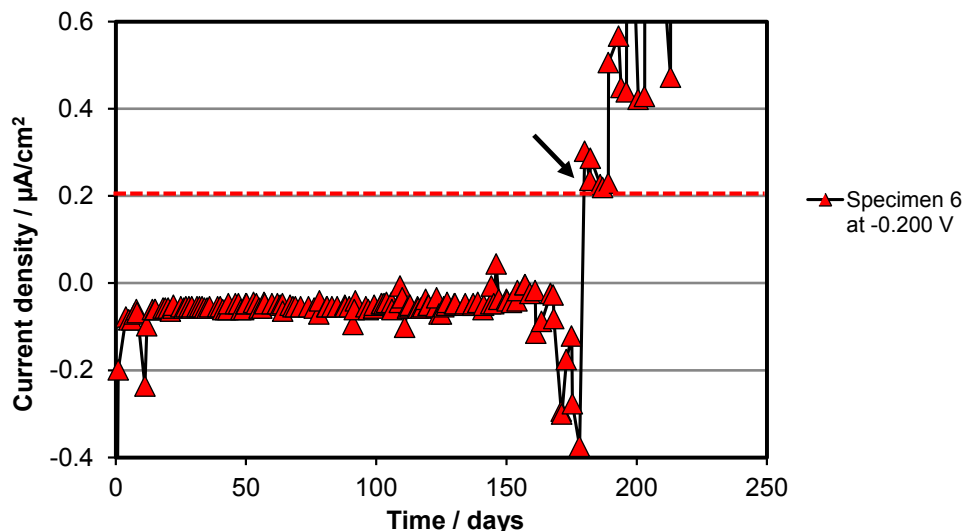

Figure 5: Current density with respect to time for a specimen cathodically polarized at -0.200 V

Chloride ion content at rebar trace

Once activation was confirmed, the specimen was removed from the experimental setup and sliced with a masonry saw on the sides until reaching approximately ~3 mm. (~1/8 in) away from the rebar. A chisel and hammer were then used to break the specimen into two halves. The top part of the specimen was then wedged away from the rebar exposing the rebar trace for the concrete-rebar interface closest to the pond (see Figure 6). The rebar trace was milled using a masonry drill 0.375 in (1 cm) diameter. The milling depth was ≤ 2 mm, and normally 9 grams of concrete powder were collected avoiding regions where corrosion products were observed. The concrete powder was analyzed for chloride ion concentration following the FDOT[2] FM5-516 "Florida Method of Test for determining Low-Levels of Chloride in Concrete Raw Materials", whereby 3-gram samples are tested in triplicate and the results averaged for a reported result (Table 1).[13]

When specimen 7 was processed, large amounts of corrosion products were observed along the concrete rebar trace; and as a result, an insufficient amount of concrete powder (only about 1/3) was collected to meet the recommendation given in the FDOT FM5-516.[13] Consequently, the reported result for that specimen was for a single (not average of triplicate tests) value and subject to corresponding uncertainty. That value was unusually large and suggestive of an artifact.

---

[2] Florida Department of Transportation (FDOT), 605 Suwannee Street Tallahassee, FL 32301

Chloride ion content at the concrete ponding surface

The chloride content at the concrete ponding surface C_S was determined for selected specimens following a similar procedure as that indicated above for the trace. The results were 20.2 kg/m³ and 22.4 kg/m³ for specimens 2 and 3, respectively. The average value, 20.2 kg/m³, was used as the fixed C_S value for all specimens in the calculations explained in the next section.

Figure 6: Reinforced concrete specimen after autopsy.

Chloride corrosion threshold determination

The procedure yielded the chloride ion concentration C_{TR} at the time of specimen removal t_R. An adjustment for time delay was conducted to estimate the concentration C_T at the declared time of activation (t_A). The adjustment was calculated assuming simple diffusion in a semi-infinite[(3)] plane sheet with invariant Cs, Co and D (Equation 2), but correcting for the presence of the steel bar (diameter Φ) with clear cover X_C as described in a computational investigation by Kranc et al.[14] That work shows that for the above conditions the concentration C after a time of exposure t at the point of the rebar surface closest to the external surface is given by

$$C = C_S \left(1 - erf \frac{X_C}{2\sqrt{Dt/Tf}}\right) \qquad (2)$$

where T*f* is a derating factor that is a function of the ratios Φ / X_C and C/C_S (note the formulation as expressed in Equation 2 is implicit on C). For the present case Φ/ X_C = 0.77, a fixed value. Processing accordingly the graphic solutions to Equation 2 given by Kranc for that ratio value shows that Tf can be approximated by:[14]

$$Tf = -0.65\frac{C}{C_S} + 0.792 \qquad (3)$$

Using the global values of Cs and Xc and taking for each specimen C=C_{TR} and T=t_R, the corresponding value of D was calculated by clearing it from Equation 2, with results shown in Table 1. As shown there, the results for specimens 1-6 were quite consistent with each other (average 5.14E-08 cm²/s, standard deviation 1E-08 cm²/s) and in the expected range for a highly permeable concrete as used here. Once the values of D were obtained, solving numerically equations 2 and 3 with t=t_A, the value C=C_T was obtained, corresponding to the adjusted value of the threshold for the specimen and listed in Table 1 as well.

Due to the uncertainty associated with the chloride content of specimen 7, two alternative values of C_T are presented. The first involves no adjustment procedure so C_T was taken to be nominally equal to C_{TR}. In the second, the average value of D (D_{AVG}) obtained for specimens 1-6 was used together with

---

[(3)] The domain is actually of finite thickness, but since it is about 3 times greater than X_C, the behavior at the relatively early stages considered here approximates conditions in a semi-infinite domain.

Equations 2 and 3 to obtain a numerical estimate of C_T for specimen 7. Both values are shown as a range in Table 1.

Five of the cathodically polarized specimens did not experience corrosion activation up to day 600, as mentioned earlier. Exposure continues, but a nominal bounding lower value of C_T was obtained following the same method as that used to obtain the second alternative for specimen 7.

Table 1
Experimental and calculated results

Specimen number	Potential / V	t_A / days	t_R / days	C_{TR} / kg m^{-3}	D / cm^2 s^{-1}	C_T / kg m^{-3}	C_T / % by wt. of cement
1	-0.1	161	180	4.10	5.38E-08	3.45	0.76
2	-0.1	243	250	6.20	5.34E-08	6.01	1.32
3	-0.1	297	327	6.02	3.98E-08	5.37	1.18
4	-0.2	335	347	6.06	3.77E-08	5.82	1.28
5	-0.2	213	222	6.64	6.40E-08	6.35	1.39
6	-0.2	189	222	6.18	5.99E-08	5.09	1.12
7	-0.4	320	347	20.6	-	7.7*-20.6	1.7*-4.5
8	-0.4	600	-	-	D_{AVG}	11.9**	2.61**
9	-0.4	600	-	-	D_{AVG}	11.9**	2.61**
10	-0.6	600	-	-	D_{AVG}	11.9**	2.61**
11	-0.6	600	-	-	D_{AVG}	11.9**	2.61**
12	-0.6	600	-	-	D_{AVG}	11.9**	2.61**

Notes:
*Value of C_T estimated using average value of D (D_{AVG}=5.14E-08 cm^2/s) from specimens 1 to 6
**Lower bound values of C_T estimated with D_{AVG} for specimens non-activated specimens

Findings in the context of related investigations

Figure 7 shows the present results in a plot that contains previous data on the C_T-E relationship reported by Presuel-Moreno et al and updated by Sánchez and Sagüés.[4,9] In the x-axis C_T is expressed in total chloride content by weight of cement. The vertical dashed blue line indicates the maximum limit of chloride ion concentration at the rebar surface based on the C_S and CF values for the current tests. The present C_T findings experimentally estimated following the full established procedure, represented by the yellow diamonds (results for specimen 7 are shown as a range), are consistent with previous work. The yellow circles correspond to the estimated data of the non-activated specimens and black arrows pointing to the right hand side indicate that that C_T estimated at day 600 is expected to increase since specimens have not activated under that potential.

The dashed red line is traced per Equation 1 and corresponds to a β_{CT} slope of 0.550 V, E_{T0}: -0.100 V (SCE) and C_{T0}: 0.5% Cl$^-$ ion by cement weight, which are parameter values proposed in previous work by the authors as likely indication of the boundary between active and passive conditions at the various potentials and chloride contents.[2,7] The present results are satisfactorily in agreement with that proposal. The emerging data continue to suggest that the slope β_{CT} is rather steep, indicative that cathodic prevention may require a significant amount of cathodic polarization to be effective. Results and conclusions are preliminary since the investigation is still in progress. It is noted that for simplicity extrinsic effects occurring on the concrete surrounding the steel surface, such as migration, convection, OH$^-$ ion generation, air voids, cement hydration, etc. were not taken into consideration in this investigation. Those factors merit inclusion in subsequent analysis.
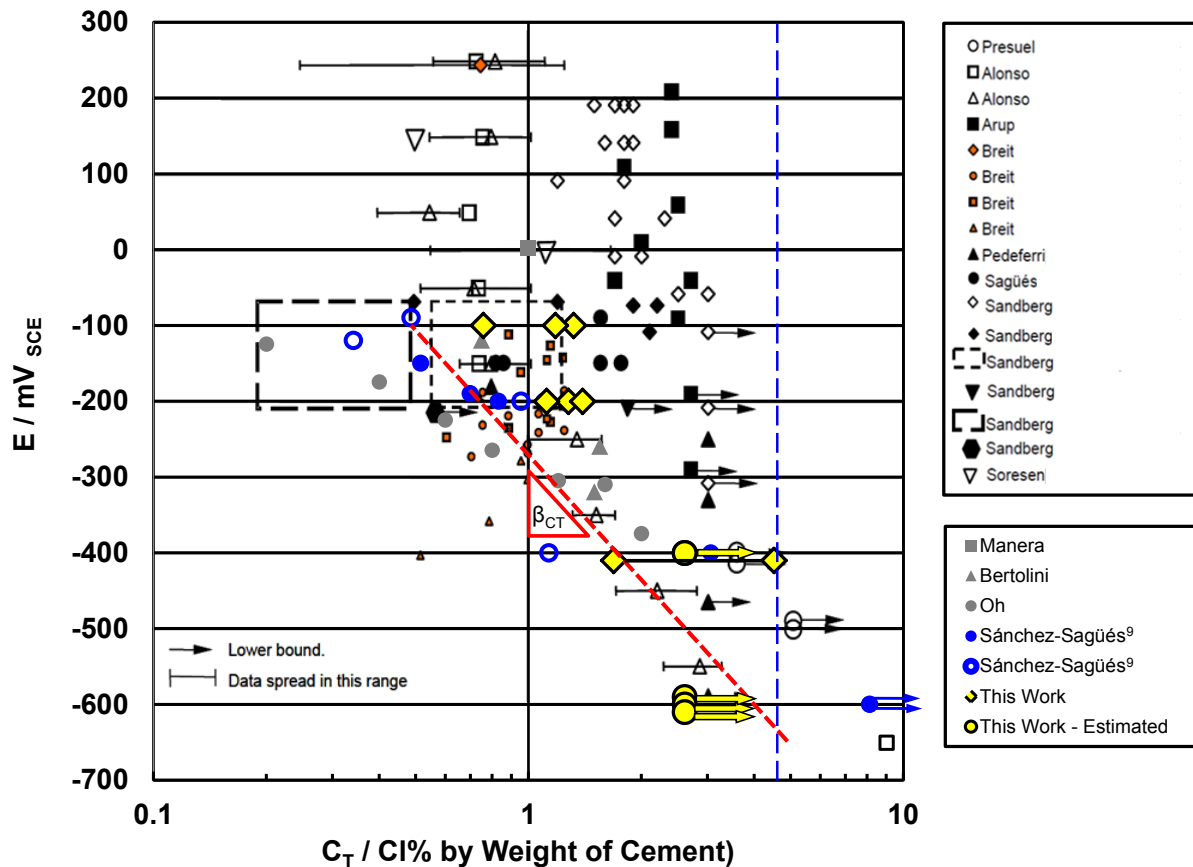
Figure 7. Chloride Threshold vs Steel Potential. Initial compilation by Presuel-Moreno et al.[4] (black symbols); updated by Sánchez and Sagüés[9] (gray and blue symbols). This work: yellow diamonds and yellow circles. See text for further details. Some symbols are slightly offset for clarity.

CONCLUSIONS

Experimental assessment focused on chloride threshold dependence on steel potential was successfully expanded to include specimens in concrete and with considerably large area of exposed metal.

The C_T values, obtained from the open circuit potential and polarized conditions at -0.200V (SCE) , and bounding values for specimens that have not yet activated, were consistent with values in the literature reported for smaller specimens in mortar.

Emerging results continue to be consistent with a rather steep value of the cathodic prevention parameter β_{CT}.

AKNOWLEDGEMENT

This investigation was supported by the Florida Department of Transportation. The opinions and findings stated here are those of the authors and not necessarily those of the funding agency.

REFERENCES

1. P. Pedeferri, 2002, Prevention of Corrosion in Concrete, Keynote, 15 International Corrosion Congress 15thICC 2002, September 23 – 27, Granada Spain.
2. C. Alonso, M. Castellote, and C. Andrade, Chloride threshold dependence of pitting potential of reinforcements. Electrochimica Acta, 2002. 47(21): p. 3469-3481.
3. U. Angst, et al., Critical chloride content in reinforced concrete - A review. Cement and Concrete Research, 2009. 39: p. 1122-1138.
4. F.J. Presuel-Moreno, A.A. Sagüés, and S.C. Kranc, Steel Activation in Concrete Following Interruption of Long-Term Cathodic Polarization. Corrosion, 2005. 61(5): p. 428-436.
5. A.A. Sagüés, and S.C. Kranc. Quantitative Corrosion Damage Function for Reinforced Concrete Marine Substructure. in 3rd. NACE Latin-American Region Corrosion Congress. 1998. Cancun, Mexico: NACE International.
6. A.A. Sagüés, S.C. Kranc and K. Lau, Modeling of Corrosion of Steel in Concrete with Potential-Dependent Chloride Threshold, in 17th International Corrosion Congress 2008, NACE International: Las Vegas, NV.
7. A.A. Sagüés, S.C. Kranc, and K. Lau, Service Life Forecasting for Reinforced Concrete Incorporating Potential-Dependent Chloride Threshold, in NACE Corrosion 2009, NACE International: Atlanta, GA. p. 22.
8. A.N. Sánchez, and A.A. Sagüés, Potential-Dependent Chloride Threshold in Reinforced Concrete Damage Prediction – Effect of Activation Zone Size. in NACE Corrosion 2013. Orlando, FL: NACE International.
9. A.N. Sánchez, and A.A. Sagüés, Chloride Threshold Dependence on Potential in Reinforced Mortar. in NACE Corrosion 2012. Salt Lake City, UT: NACE International.
10. L. Li and A.A. Sagüés, Chloride Corrosion Threshold of Reinforcing Steel in Alkaline Solutions-Effect of Specimen Size. Corrosion, 2004. 60: p. 195-202.
11. L. Basheer, J. Kropp, and D.J. Cleland, Assessment of the durability of concrete from its permeation properties: a review. Construction and Building Materials, 2001. 15(2–3): p. 93-103.
12. ASTM G109-07 Standard Test Method for Determining Effects of Chemical Admixtures on Corrosion of Embedded Steel Reinforcement in Concrete Exposed to Chloride Environments, 2007.
13. Florida Method of Test for Determining Low-Levels of Chloride in Concrete and Raw Materials" (FM 5-516). Florida Department of Transportation. 2009.
14. S.C. Kranc, A.A. Sagüés and F.J. Presuel-Moreno, Decreased Corrosion Initiation Time of Steel in Concrete due to Reinforcing Bar Obstruction of Diffusional Flow., ACI Materials Journal, Vol. 99, p.51, 2002